J Mol Model (2013) 19:139–149
DOI 10.1007/s00894-012-1529-6

ORIGINAL PAPER

Theoretical design study on photophysical property on oligomers based on spirobifluorene and carbazole-triphenylamine for PLED applications

Xiao-Hua Xie · Wei Shen · Rong-Xing He · Ming Li

Received: 11 February 2012 / Accepted: 5 July 2012 / Published online: 25 July 2012

Abstract The photophysical properties of five blue light-emitting polymers based on spirobifluorene applied in polymer light-emitting diodes (PLED) materials have been studied by quantum chemistry. In order to understand the intrinsic reasons for the different performances displayed by the polymers, we carried out density functional theory (DFT) and Marcus theory investigations on their oligomers in terms of structure and properties stability, absorption and emission properties, and carrier injection and transport properties. Especially, some important parameters which had not been reported to our knowledge were given in this contribution, such as the ionization potentials (IPs), electron affinities (EAs), reorganization energies (λ), k_e/k_h (the ratio between the electron transfer rate (k_e) and hole transfer rate (k_h)), and the radiative lifetimes (τ). The main results indicate that the co-oligomers of PCC-1, PCC-2, and PCC-3 with push-pull interactions produced by the existing D-A segments have better carrier injection and transport properties than the oligomers of PSF and PCF. Especially PCC-2 co-oligomer, its large radiation lifetime (7.46 ns) and well balanced and adequate carrier transport guarantee its champion performance for PLED. The calculated results coincide with the experimental ones. Besides, PNF structurally similar to PCC-2 has similar photoelectric properties to PCC-2 in theory, and the fluorescence emission of PNF co-oligomer is superior to PCC-2 co-oligomer. Therefore, we predict that PNF is a promising candidate for PLED.

Keywords PLED · Carrier mobility · Copolymer · DFT

Introduction

Polymer light-emitting diodes (PLEDs) as a branch in OLEDs have attracted extensive interest due to their full-color, low voltage, self-luminous, fabricating ultrathin, large-area display, fast response, and simple process [1, 2]. High performance blue, green, red, and white light-emitting polymers are required to realize PLED-based displays, whereas only a few blue light-emitting polymers show good performance in comparison with other light-emitting polymers. The simplest PLED consists of anode, cathode, and emissive layer. Under the action of driving voltage, electrons are injected from the cathode into the lowest unoccupied molecular orbital (LUMO) of the adjacent organic layer, while the anode injects holes into the highest occupied orbital (HOMO) of the organic material. Then, the electrons and holes move through the organic layer and recombine under the formation of an "exciton" capable of relaxing its excited state to the ground state by emission of light [3].

In order to promote deeper understanding of the connection between chemical structures and the optical and electronic properties of the emissive layer, and rational design of new functional materials, theoretical calculations play an important role. From the viewpoint of electronic structure, the materials used in the emissive layer should match the energy level for charge injection and should desirably possess a bipolar character, that is have both electron-transporting (ET) and hole-transporting (HT) properties, to permit the formation of both stable cation and anion radicals [4]. Quantum chemical calculations on emissive layer materials can provide important information about these properties, especially of some parameters, such as the ionization potential (IP), electron affinity (EA), and reorganization

Electronic supplementary material The online version of this article (doi:10.1007/s00894-012-1529-6) contains supplementary material, which is available to authorized users.

X.-H. Xie · W. Shen · R.-X. He · M. Li (✉)
School of Chemistry and Chemical Engineering,
Southwest University,
Chongqing 400715, China
e-mail: liming@swu.edu.cn

energies (λ). These parameters can be used to evaluate the carrier injection and transport properties, and they are difficult to be obtained from experiments. In order to be manageable, in these calculations the complex issues of a realistic condensed phase environment of the polymers are usually neglected. In order to evaluate such calculations, some key results have to be compared with experiment.

So far, polyfluorenes (PFs), polyphenylene, and polyphenylacetylene derivatives have been used as blue light-emitting materials, especially PFs are considered as promising candidates owing to their excellent thermal and chemical stability, and high photoluminescence efficiency [5–7]. In the family of PFs, spirobifluorene (SF) shows good thermal and optical stabilities due to its unusual rigid three-dimensional structure [8, 9]. In the past few years, many researchers have developed a number of PLEDs based SF via attaching different functional groups onto either fluorene unit [10, 11].

Recently, on the basis of SF, Lin et al. reported three copolymers PCC-1, PCC-2, and PCC-3 via Suzuki coupling reaction with three comonomers: 2′,7′-dibromo-2,7-bis(4′-cyanophenyl)-9,9-spirobifluorene (M1), 4-(9H-carbazol-9-yl)-4′,4″-dibromotriphenylamine (M2), and 9,9-dihexyl-fluorene-2,7-bis(trimethyleneborate) (M3) [12]. According to the different ratios of M1 and M2, copolymers PCC-1, PCC-2, and PCC-3 were gained, and two reference homopolymers PSF and PCF were also prepared for comparison, as shown in Scheme 1. In the PLED devices [12], the five polymers were fabricated as emissive layers, respectively. However, the PLED performances are obviously different (the maximum luminance for PSF, PCC-1, PCC-2, PCC-3, and PCF are 1505, 2108, 3024, 1717, and 1427 cd/m^2, respectively [12]). Why did the copolymers show better performance than homopolymers, and why was PCC-2 the champion polymer for PLED performance? In order to locate the intrinsic reasons, we carried out density functional theory (DFT) calculations on the oligomeric electronic structures, absorption and emission spectra, frontier molecular orbital energies (FMOs), energy gaps (E_g), IPs, EAs, λ, k_e/k_h (the ratio between the electron transfer rate (k_e) and hole transfer rate (k_h)), and the radiative lifetimes (τ). Through the above parameters of oligomers, we analyzed some determined properties of polymers for PLED in detail, such as the structure and properties stability, absorption and emission properties, carrier injection and transport properties which have not been reported to our knowledge (Marcus theory [13] was employed to describe the dynamics of charge transfer properties). In addition, we replaced 9,9-dihexyl-9H-fluorene wiht 9-butyl-9H-carbazole in PCC-2 to design a new polymer PNF (which has not been synthesized yet), and then theoretically investigated the potential of PNF as emissive layer through comparing the oligomeric properties with PCC-2.

This paper is organized as follows. In Sect. II, we described the computational methods to obtain the geometries and density topological analyses. The basic theory used in the calculation carrier mobilities was also discussed. In Sect. III, we reported the structural and properties stability, absorption and emission spectra, carrier injection abilities and carrier transport properties as well as the experimental observations. Concluding remarks were given in Sect. IV.

Calculation methods

In this paper, density functional theory (DFT) and time-dependent DFT (TD-DFT) [14] are used to obtain the qualitative features of all the compounds at B3LYP/6-31G (d) level [15, 16]. All the optimized structures have no imaginary frequencies at the present level, which suggests that all the optimized structures are the global minima on the potential energy surface. The absorption spectra of all the oligomers were computed by TD-B3LYP/6-31G (d) method, whereas, the emission spectra are computed at TD-B3LYP/6-31G level due to the large amount of atoms. All the calculations are carried out by Gaussian 09 package [17]. In addition, atom in molecule **(AIM)** [18] theory is employed to examine the density topological analyses of the oligomers, and the nucleus-independent chemical shift **(NICS)** [19] is also calculated at the B3LYP/6-31G (d)

Scheme 1 Detailed polymeric manner for polymers

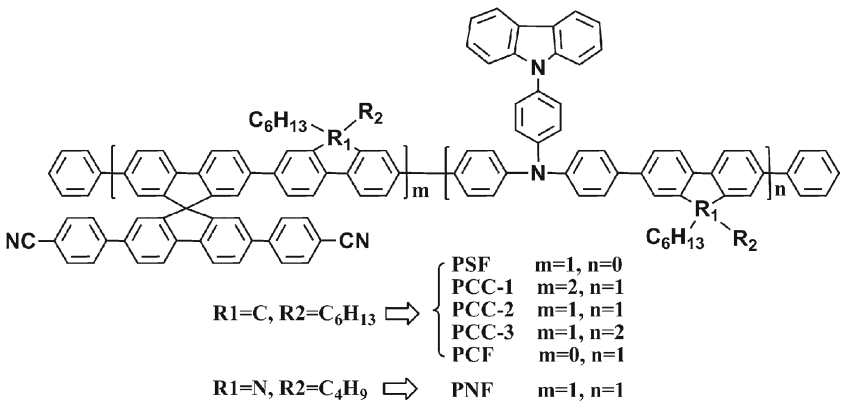

level. The NICS method possesses the merit that it allows the evaluation of aromaticity, antiaromaticity, and nonaromaticity of single-ring systems and individual rings in polycyclic systems (local aromaticities) [20]. In this work, NICS is defined as the negative of the magnetic shielding at a ring critical point (RCP) which is gained from the AIM analyses. Furthermore, the bonding characteristics are investigated by natural bond orbital (**NBO**) theory [21–24]. The density of state (DOS) and projected density of state (PDOS) are performed and their graphs are obtained from GaussSum 1.0 [25, 26]. The charge transfer rate (K) can be described by Marcus theory [27–29] via the following equation when the charge transfer is a self-exchange transfer process:

$$K = \left(V^2/\hbar\right)(\pi/\lambda k_B T)^{1/2} \exp(-\lambda/4k_B T) \quad (1)$$

Here, T is the temperature, k_B is the Boltzmann constant, λ represents the reorganization energy due to geometry relaxation accompanying charge transfer, and V is the electronic coupling matrix element (transfer integral) between the two adjacent species dictated largely by orbital overlap. It can be seen from Eq. 1 that there are two major parameters that determine the charge transfer rate: (i) V, which needs to be maximized, and (ii) λ, which needs to be small for significant transport. In order to investigate V, crystal data in general are required [30–33]. However, the studied polymers may be noncrystal, and the electronic coupling matrix element value is very limited [34–36]. Thus, we focus on their reorganization energies to investigate their charge transport properties. Generally, the reorganization energy is determined by the fast change of the molecular geometry when a charge is added or removed from a molecule (the internal organization energy λ_{int}) and represents the variations in the surrounding medium due to the polarization of effects (the external reorganization energy λ_{ext}) [37]. Since the studied polymers are used as emissive polymers in the solid film, the dielectric constant of the medium for the polymers is low. Therefore, we only focus on the discussion of the λ_{int} (reflects the geometric changes in the molecules when going from the neutral to the ionized state and vice versa) of the isolated active organic π-conjugated systems due to ignoring any environmental relaxation and changes in this paper. Hence, the electron reorganization energy (λ_e) and hole reorganization energy (λ_h) values can be calculated by Eqs. 2 and 3 [38]:

$$\lambda_e = (E_{na} - E_{nn}) + (E_{an} - E_{aa}) \quad (2)$$

$$\lambda_h = (E_{cn} - E_{cc}) + (E_{nc} - E_{nn}) \quad (3)$$

Here, E_{cn} (E_{an}) is the energy of cation (anion) calculated with the optimized structure of the neutral molecule. Similarly, E_{cc} (E_{aa}) is the energy of the cation (anion) calculated with the optimized cation (anion) structure and E_{nc} (E_{na}) is the energy of the neutral molecule calculated at the cationic (anionic) state. Finally, E_{nn} is the energy of the neutral molecule at the ground state. When neglecting the effect of V, the ratio between the electron transfer rate (k_e) and hole transfer rate (k_h) can be obtained according to Eq. 4:

$$\frac{k_e}{k_h} = A\left[\left(\frac{\lambda_e}{\lambda_h}\right)^{1/2} \exp\left(\frac{\lambda_e - \lambda_h}{4K_B T}\right)\right] \quad (4)$$

Here, A is a prefactor.

Results and discussion

The sketch maps of the studied polymers are depicted in Scheme 1. With regard to PNF co-oligomer, we replaced n-hexyl with n-butyl to decrease calculation cost without affecting the results [39]. The optimized structures of studied oligomers are plotted in Scheme 2.

Figure 1 showed the total density of states (DOS) and projected density of states (PDOS) to more easily and vividly observe the varieties of the highest occupied molecular orbitals (HOMOs) and the lowest virtual molecular orbitals (LUMOs), and energy gaps. As shown in Fig. 1, in the co-oligomers (the oligomers of PCC-1, PCC-2, PCC-3, and PNF), the HOMOs are mainly consisted of PSF unit (solid line), whereas the LUMOs are mainly contributed by PCF unit (dash line). In other words, PCF unit is mainly the acceptor (A) segment, and PSF unit is mainly the donor (D) segment. Therefore, PCC-1, PCC-2, PCC-3, and PNF can be simply expressed as the following forms: D-A-A, D-A, D-D-A, and D-A. Further, the HOMO and LUMO orbital diagrams in Fig. 2 can show the specifical locations of the electronic cloud distribution of FMOs. It can be seen from Fig. 2, the electronic loud distribution of LUMO in all the co-oligomers localizes on the side chain (cyano-phenyl-fluorene), while that of HOMO localizes near the carbazol-triphenylamines, namely, the acceptors are mainly contributed by cyano-phenyl-fluorene groups, and the donors are mainly contributed by carbazol-triphenylamines.

Structure and properties stability

Stability is the prerequisite of material. First, we investigate the structure stability of studied oligomers. The dihedral angles in Table 1S in supporting information are smaller than 37 °C, which suggests that the twist of all the studied oligomers is small. Hence, the planarity of PCC-2 is the best in all studied polymers due to the

Scheme 2 The stereograph of optimized oligomers

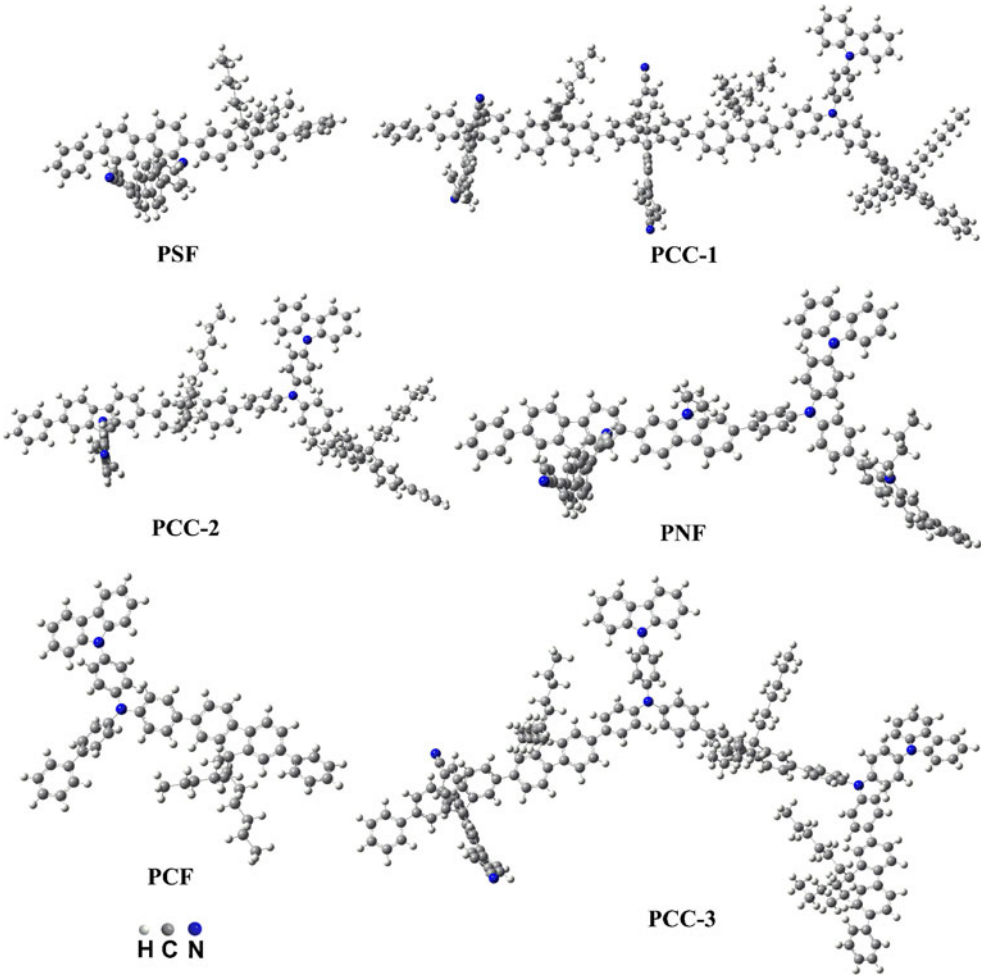

smallest dihedral angle of its co-oligomer. The central bond is as a bridge linking the donor and acceptor as shown the bonds signed with E in Fig. 1S (in supporting information), and its properties can reflect and influence the properties of the polymers. Herein, some properties of the central bonds were listed in Table 1S. The data of bond lengths, Wiberg bond indexs (WBIs), and configurations for bonding orbitals of central bonds manifest that central bonds contain π bond components.

Since NICS can distinctly and simply monitor the condition of ring currents, it is widely used to express the aromaticity of molecules. Systems with significantly negative NICS values are aromatic and systems with strongly positive NICS values are anti-aromatic, and non-aromatic cyclic systems should therefore have NICS values close to zero [19, 40–42]. Generally, NICS is computed at a ring center, namely in the position of RCP. The NICS values of the studied polymers are calculated at B3LYP/6-31G (d) level and given in Table 2S in supporting information, and the positions of all the rings in the molecular system are shown in Fig. 1S. From Table 2S, we can see that all the studied rings (along the polymeric axis) have large ring current due to the negative NICS. However, all the ring currents of calculated benzene rings in the work are smaller than that of single benzene ring (NICS, -9.7 at B3LYP/6-31G (d) level), which results from the electrons delocalizing to the whole studied molecules and decreases the local ring current, namely, the studied oligomers are conjugated systems. Moreover, the b3, b4, c3, c4 rings in PNF co-oligomer are close to the electron-rich nitrogen atom, so their ring currents are more negative in comparison with the single benzene ring. Further, the electronic cloud distribution of FMOs in Fig. 2 indicates that all the studied polymers are favorable π-conjugated systems. Therefore, the studied oligomers are systems with favorable structural stability.

In the work, we analyzed the antioxidation properties and thermal stability to investigate the properties stability. Generally, high HOMO energy level easily results in electron escaping, and effective antioxidant property requires lower HOMO energy level than -5.27 eV (below the air oxidation threshold, ca. -5.27 eV) [43]. The HOMO and LUMO energies were calculated at B3LYP/6-31G (d) level in this study. The calculated HOMO and LUMO energies, and energy gaps as well as the experimental values are listed in

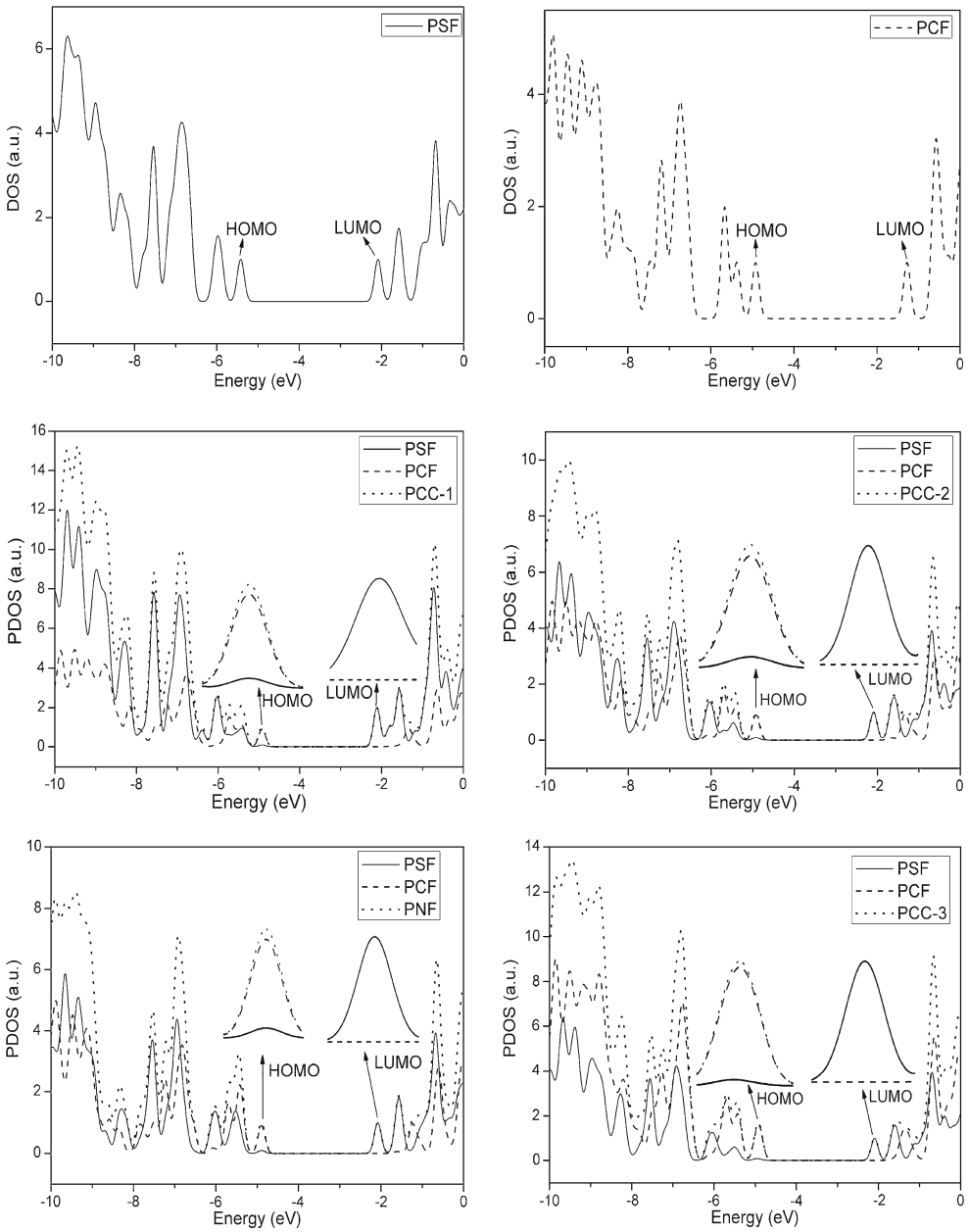

Fig. 1 DOS and PDOS of the oligomers

Table 1. From Table 1, we can see that the change trend in orbital energies matches well with the experimental results, and all the HOMO energy levels of experimental polymers are around the air oxidation threshold, especially PSF has the strongest antioxidation properties among the studied polymers due to the lowest experimental HOMO energy level. It is noteworthy that the calculated energy gaps of co-oligomers agree with the experimental ones, which suggests that the co-oligomers are already sufficient for the polymers to perform representative calculations. In order to obtain the thermal stabilities, we investigate the bond dissociation energy (*BDE*) of central bonds in oligomers, as summarized in Table 1S. *BDE* is considered as the enthalpy changes in the reaction $A-B \rightarrow A\bullet + B\bullet$ at 298 K and 1.013×10^5 Pa. The data in Table 1S indicate that most of the *BDE* values are larger than 317 kJ mol^{-1}, and the values obviously increase with the increased ratios of SF, which are consistent with the experimental thermal properties evaluated by thermo gravimetric analysis (TGA) [12].

We conclude that all the studied oligomers are stable in structures and environment, especially the co-oligomers containing a larger proportion of SF, which coincides with the experimental results. As to the designed polymer, PNF, its oligomer has the same structural and properties stability as PCC-2 oligomer due to the same planarity, conjugation, FMO energy levels, energy gaps and *BDE* of central bond. Thus, PNF is a candidate for material with structural and properties stability as PCC-2.

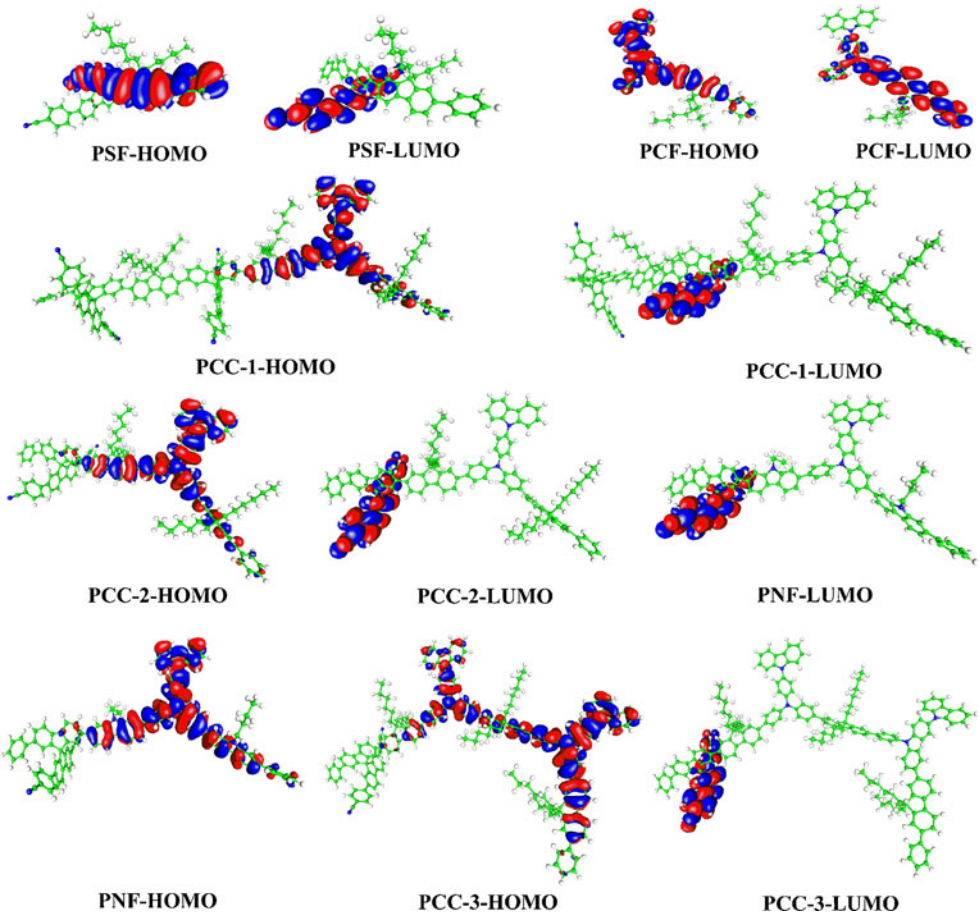

Fig. 2 HOMO and LUMO orbital diagrams for oligomers

Absorption spectra and emission spectra

The simulated absorption spectra of studied oligomers by TD-DFT/B3LYP functional with 6-31G (d) basis set are given in Fig. 3b. The effect of the solvent (toluene) within polarizable continuum model (PCM) [44] is taken into account during the calculation. The experimental absorption spectra in toluene solution of the experimental polymers are shown in Fig. 3a for comparison. From Fig. 3b, we can see that the absorption bands of the co-oligomers of PCC-1, PCC-2, and PCC-3 are red-shifted with the increasing ratio of carbazole-triphenylamines (PCC-1: 390, PCC-2: 417, PCC-3: 420), which is consistent with the experimental results (PCC-1: 360, PCC-2: 366, PCC-3: 371) in spite of that the calculated maximized absorption wavelengths (λ_{abs}^{max}) are larger than the measured ones. An important factor that the calculated data deviate from the experimental values could be ascribed to the different frequencies between experiment and calculation.

From PCC-1 unit to PCC-3 unit, the increased ratios of electron-rich triphenylamine enlarge the π systems and reduce the energy level spacing, and then result in the above-mentioned changes in the electronic spectra. The transition energies, oscillator strengths, and configurations relevant to the singlet excited states in each molecule are listed in Table 3S, accompanied by the experimental results. The electron transitions of some main excited states are depicted in Fig. 4. As shown in Table 3S and Fig. 4, the main configurations with the maximum wavelength in co-oligomers belong to single electron transitions mainly assigned to $\pi \rightarrow \pi^*$ transition. In Fig. 4, the charge transfer of PSF unit occurs in the fluorene units along the main chain in 370 nm, while the charges transfer from carbazol-triphenylamines to fluorene unit in PCF unit. In the co-oligomers, the charge transfer

Table 1 Frontier molecular orbital energy levels, and energy gaps (Eg), as well as experimental data. All energies are in eV

Polymer	HOMO		LUMO		Eg	
	exp[a]		exp[a]		exp[a]	
PSF	−5.71	−5.42	−2.94	−2.08	2.77	3.34
PCC-1	−5.27	−4.93	−2.40	−2.12	2.87	2.81
PCC-2	−5.26	−4.92	−2.40	−2.09	2.86	2.83
PCC-3	−5.26	−4.87	−2.39	−2.09	2.87	2.78
PCF	−5.26	−4.91	−2.38	−1.30	2.88	3.61
PNF	–	−4.9	–	−2.08	–	2.82

[a] The data are from [12]*

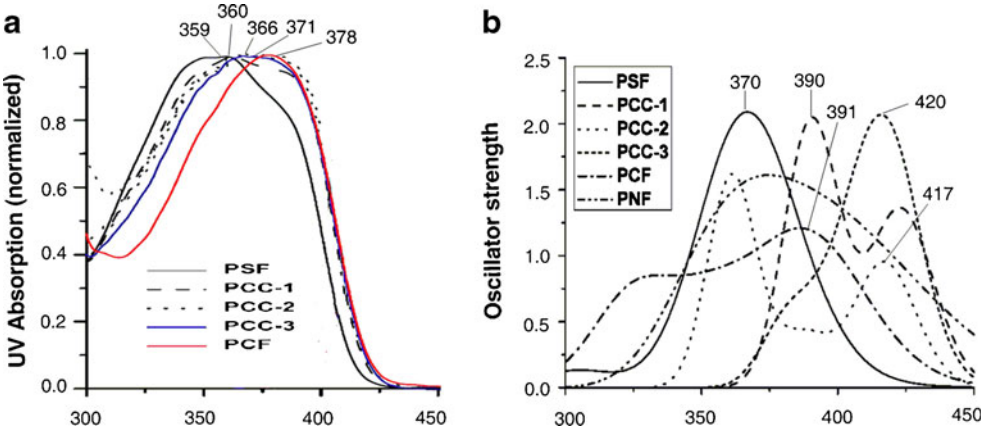

Fig. 3 (**a**) Experimental absorption spectra of polymers in toluene solution [12] and (**b**) simulated absorption spectra of oligomers (including PNF) in toluene solution

occurs from carbazol-triphenylamines (donor segment) to the SFs (acceptor segment) along the main chains. Nevertheless, the side chains as the main contributor to LUMO, cyanophenyl-fluorene, hardly participate in the electron transition in the maximized absorption.

As shown in Fig. 3b, we also simulated the absorption spectrum of PNF oligomer in toluene solution by TD-DFT/B3LYP functional with 6-31G (d) basis set for comparison with PCC-2. The transition energies, oscillator strengths, and configurations relevant to the singlet excited states in each molecule are also listed in Table 3S, accompanied by the electron transitions of λ_{abs}^{max} depicted in Fig. 4. As shown in Table 3S, the λ_{abs}^{max} of PNF oligomers (411 nm) is close to that of PCC-2 oligomer (417 nm), and the oscillator strengths and main configurations at the lowest excited states are similar. In comparison with the charge difference densities in Fig. 4, we find that the charge transfer in PNF oligomer occurs from carbazol-triphenylamine to SF, whereas the carbazole in PCC-2 hardly participates in charge transfer. Through comparing the electronic spectra between PNF and PCC-2 oligomers, we predict that the λ_{abs}^{max} of polymer PNF is between 359–366 nm, and they have the same absorption properties.

In order to obtain the emission spectra properties, we calculated the emission spectra in toluene solution of all the studied oligomers at TD-B3LYP/6-31G level. Analogous calculations for emission spectra based on hybrid DFT functions have been implemented [45–47]. Unfortunately, we were only able to obtain the emission spectra properties of the oligomers of PSF, PCC-2, PCF, and PNF. As shown in Table 2, it can be seen that the emission peaks with large oscillator strength are all assigned to $\pi \rightarrow \pi^*$ character arising from HOMO → LUMO transition. The calculated values of the vertical fluorescence wavelength for PSF, PCC-2, and PCF oligomers are located at 455, 442, 469 nm, respectively, thereinto, only the theoretical fluorescence wavelength of PCC-2 is analogous to the experimental one.

The Stokes shifts of PSF, PCC-2, and PCF measured by experiment are 55, 83, and 47 nm [12], it may be explained that these polymers have large change of the structures in ground and excited states, however, the theoretical Stokes shifts for their oligomers are 85, 25, and 78 nm due to the deviations of the calculated λ_{abs}^{max} and λ_{em} values. Further, the radiative lifetimes have been computed for spontaneous emission using the Einstein transition probabilities according to the formula (in au) [48, 49]:

$$\tau = \frac{c^3}{2(E_{Flu})^2 f} \tag{5}$$

Here, c is the velocity of light, E_{Flu} is the excitation energy, and f is the oscillator strength (in Table 2). The calculated lifetimes τ for the oligomers of PSF, PCC-2, and PCF are 3.06, 7.22, 4.28 ns, respectively, PCC-2 oligomer has the largest τ, which is in accordance with the largest experimental Stokes shift of PCC-2. From ground to excited states, PCC-2 has larger change of structures than PSF and PCF, and the changed structure of PCC-2 has smaller energy level spacing relative to the former structure, which results in smaller excitation energy for PCC-2. In accordance with Eq. 5, the smaller excitation energy and f, the larger τ. Therefore, the largest radiative lifetime of PCC-2 oligomer should be responsible for the better luminance of its polymer.

As to PNF co-oligomer, combining Table 2 and Table 3S, we can see that the theoretical Stokes shift of PNF co-oligomer is 22 nm, which is the same as the theoretical Stokes shift of PCC-2 co-oligomer. The τ value (vertical fluorescence) of PNF co-oligomer is 7.67 ns that is 0.45 ns larger than PCC-2 co-oligomer due to the small f of PNF co-oligomer, though the excitation energy of PNF co-oligomer is 0.05 eV larger than that of PCC-2 co-oligomer. The large τ of PNF co-oligomer is bound to benefit the photoelectric properties of its polymer.

Carrier injection

The IP and EA are well-defined properties that can be calculated by DFT to estimate the energy barrier for the injection of carrier (hole and electron) into the emissive layer. The calculated IPs, EAs, both vertical (V; at the geometry of the neutral

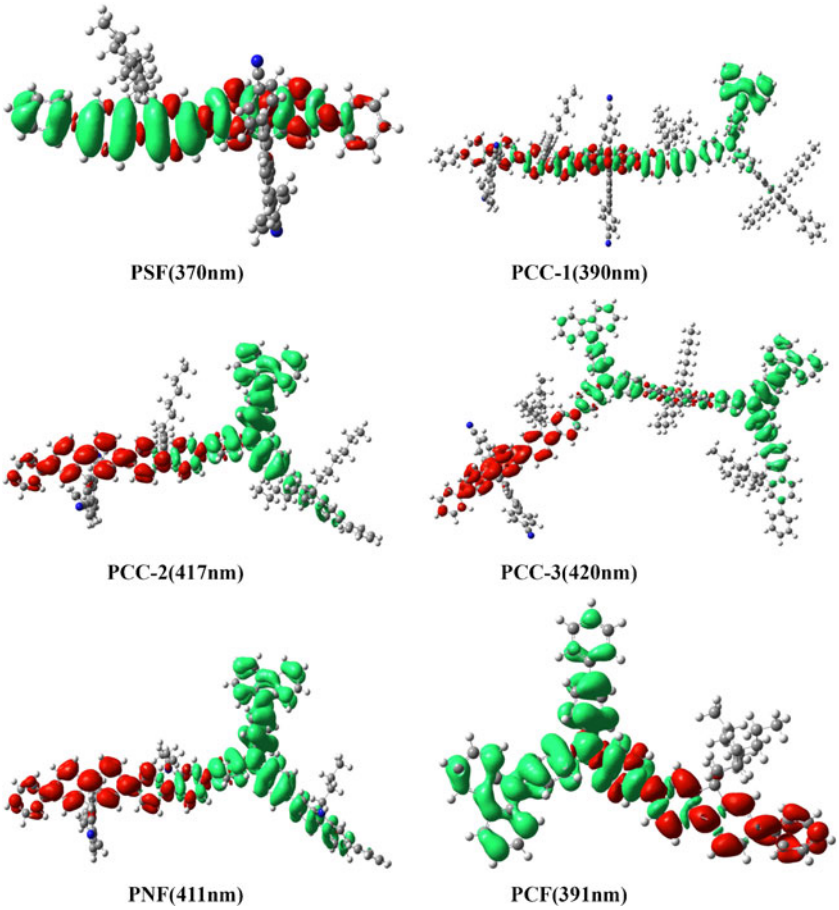

Fig. 4 Charge difference densities of the main electronic excited states of each molecule, where the green and red colors stand for the hole and electron, respectively

molecule) and adiabatic (A; optimized structure for both the neutral and charged molecule), and the extraction potentials (HEP and EEP for the hole and electron, respectively) that refer to the geometry of the ions [50, 51].

One general challenge for the application of molecules in OLEDs is achievement of high EA molecules for improving the electron injection/transport and low IP molecules for better hole injection/transport. In the work, the studied polymers are emissive layers, the balance of electron/hole injection/transport through the device is critical, besides, it is better that the studied polymers have small IPs and large EAs in the meantime. Also, it has been experimentally proved that Mes_2B[*p*-4,4′-biphenyl-NPh(1-naphthyl)] (BNPB) is a good trifunctional molecule [52]. The calculated IPs and EAs of studied oligomers are given in Table 3. From Table 3, it is can be seen that the IPs of the oligomers of PCC-1, PCC-2, PCC-3, and PCF, are smaller than that of BNPB (6.09 eV) at the same level [53], which suggests that the above molecules have smaller barriers than BNPB in the losing electrons process. Obviously, the oligomers of PSF, PCC-1, PCC-2, and PCC-3 are easier to accept an electron than BNPB due to their larger EAs than BNPB (0.74 eV) [54] at the same level, which indicates that the above oligomers obtain electrons more easily than BNPB. In summary, the co-oligomers, PCC-1, PCC-2, and PCC-3 have bipolar characters, whereas the oligomers of PSF and PCF

Table 2 Emission spectra obtained by TD-DFT method for studied oligomers at the B3LYP/6-31G optimized geometries

	Electronic state change	λ_{em} (nm)	λ_{em}^{exp} (nm)	*f*	τ (ns)	Excitation energies (eV)	Main configuration and coefficient
PSF	$S_6 \rightarrow S_0$	455	414	2.47	3.06	2.72	HOMO → LUMO + 1 0.99
PCC-2	$S_3 \rightarrow S_0$	442	449	0.98	7.22	2.81	HOMO → LUMO + 2 0.89
PCF	$S_2 \rightarrow S_0$	469	425	1.87	4.28	2.64	HOMO → LUMO 0.98
PNF	$S_4 \rightarrow S_0$	433	–	0.89	7.67	2.86	HOMO → LUMO 0.69 HOMO → LUMO + 2 0.89

[exp] Measured in toluene [12]

Table 3 Ionization potentials, electron affinities, extraction potentials, reorganization energies, and the ratios between the electron transfer rate (k_e) and hole transfer rate (k_h) for each molecules. All energies are in eV

Polymer	AIP	VIP	HEP	AEA	VEA	EEP	λ_h	λ_e	k_e/k_h
PSF	6.27	6.37	6.16	1.22	1.07	1.38	0.21	0.31	3.16
PCC-1	5.60	5.66	5.55	1.54	1.45	1.63	0.11	0.18	2.40
PCC-2	5.65	5.74	5.59	1.28	1.17	1.50	0.15	0.22	2.40
PCC-3	5.44	5.49	5.39	1.33	1.23	1.53	0.10	0.20	3.43
PCF	5.73	5.83	5.64	0.49	0.31	0.85	0.19	0.36	7.60
PNF	5.63	5.71	5.55	1.25	1.13	1.50	0.16	0.25	3.05

only have single polar property. Therefore, the co-oligomers are suitable as the emissive layer, since they are easily injected into electrons and holes, which is one factor of their better performances than the homopolymers.

As to the co-oligomer of PNF, from Table 3, we can see that the IP and EA values of PNF unit (AIP: 5.63, VIP: 5.71, AEA: 1.25, VEA: 1.13 eV) are slightly smaller than those of PCC-2 unit (AIP: 5.65, VIP: 5.74, AEA: 1.28, VEA: 1.17 eV). The above-mentioned results indicate that PNF co-oligomer has the same carrier injection properties as PCC-2 co-oligomer, and PNF is a promising candidate for a bipolar character material.

Charge transfer properties

Understanding the relationship between the molecular structure and the charge transport property of a material is a key point in rationalizing the experimentally observed properties of known materials and providing good candidates for the design of photoelectric materials. Herein, the reorganization energy was just the inner reorganization energy of the isolated active organic π-conjugated systems due to ignoring any environmental relaxation and changes. The calculated results of λ_e, λ_h and the ratio between the electron transfer rate and hole transfer rate (k_e/k_h) values for the investigated molecules were summarized in Table 3.

The λ_e values of the co-oligomers of PCC-1, PCC-2, and PCC-3 (0.18–0.22 eV) are smaller than that of tris(8-hydroxyquinolinato)aluminum(III) (Alq3) (λ_e =0.276 eV), a typical electron transport material [55], which results from the former with smaller barriers in structure changing due to gaining electrons. The above results indicate that their electron transfer rates may be higher than that of Alq3. On the other hand, because of smaller barriers of vibration structures of the co-oligomers in electron losing process, their λ_h values (0.10–0.15 eV) are smaller than that of N, N'-diphenyl-N, N'-bis(3-methlphenyl)-(1,1′-biphenyl)-4,4′-diamine (TPD) (λ_h=0.290 eV), which is a typical hole transport material [56], implying that their hole transfer rates may be higher than that of TPD. Whereas, the oligomers of PSF and PCF are inferior to Alq3 due to their large λ_e, moreover, their λ_e and λ_h are larger than other molecules, which results in their inferiorly balanced transport properties to other studied molecules. It is noteworthy that the push-pull interactions due to D-A are formed in the co-oligomers of PCC-1, PCC-2, and PCC-3, and the interactions can improve charge transfer, which is one of the important reasons for their superiority to PSF and PCF oligomers in carrier transport properties. Obviously, the k_e/k_h values in Table 3 indicate that PCC-1 and PCC-2 oligomers have well balanced transport properties due to their small k_e/k_h values (2.40). Therefore, well balanced and adequate transport of both injected electrons and holes are also the conditions of polymer PCC-2 obtaining good performance.

In comparison with PCC-2 oligomer, the carrier transport rates of PNF oligomer are inferior to PCC-2 oligomer at both the size and balance. However, the differences are slight, such as the λ_h of PCC-2 and PNF oligomers are 0.15 and 0.16 eV, respectively, and the λ_e are 0.22 and 0.25 eV, respectively. Hence, we conclude that the carrier transport property of PNF is similar to that of PCC-2.

In the oligomers of PSF, PCC-1, PCC-2, PCC-3, and PCF, the PCC-2 co-oligomer has well structure and properties stability, relatively small carrier injected barriers due to its small IP and EA values, larger Stokes shift (83 nm) and radiative lifetime (7.22 ns), and well balanced and adequate carrier transport due to its smaller λ_e, λ_h and k_e/k_h. The above good structural and photoelectric properties of PCC-2 co-oligomer should be responsible for the favorable performance of its polymer in PLED, while the poor carrier injection and transport properties of PSF and PCF oligomers should be responsible for the poor luminance of their polymers.

As to PNF co-oligomer, its structure and properties stability, absorption and emission spectra, and carrier transport properties are similar to those of PCC-2 co-oligomer. Moreover, PNF co-oligomer is superior to PCC-2 co-oligomer in fluorescence emission due to larger radiation lifetime (7.67 ns). Therefore, we predict that polymer PNF is a promising candidate for PLED.

Conclusions

In this contribution, density functional theory (DFT) and Marcus theory have been employed to model a series of spirofluorene derivatives, PSF, PCC-1, PCC-2, PCC-3, and

PCF, to investigate the intrinsic reasons for their different photoelectric properties in PLED. In order to design a promising candidate for PLED, we designed a new polymer PNF according to PCC-2 which had the best performance in the above five polymers, and theoretically predicted its potential as PLED material. The investigations refer to their electronic structures, absorption and emission spectra, frontier molecular orbital energies (FMOs), energy gaps (E_g), IPs, EAs, λ, k_e/k_h, and the radiative lifetimes (τ) of their oligomers. Through the above parameters, we analyzed some determined properties of the polymers for PLED in detail, such as the structure and properties stability, absorption and emission properties, carrier injection and transport properties.

The studies show the co-oligomers of PCC-1, PCC-2, and PCC-3 have better carrier injection and transport properties due to push-pull interactions produced by the existing D-A segments, and the bipolar characters of the co-oligomer guarantee their better performances than the oligomers of PSF and PCF. Especially PCC-2 co-oligomer has relatively small carrier injected barriers, larger Stokes shift (83 nm) and radiation lifetime (7.22 ns), and well balanced and adequate carrier transport, and the above-mentioned properties should be responsible for the favorable performance of its polymer in PLED, while poor carrier injection and transport properties are the main reasons for the poor luminance of PSF and PCF.

As to PNF co-oligomer, its electronic structure and photoelectric properties are similar to those of PCC-2 co-oligomer. Moreover, PNF co-oligomer is superior to PCC-2 co-oligomer in vertical fluorescence emission due to large radiation lifetime (7.67 ns). Therefore, we predict that PNF is a promising candidate for PLED.

Acknowledgments This work was supported by National Natural Science Foundation of China (Grant No.21073144), and by Ph.D. Programs Foundation of Ministry of Education of China (Grant No. 200806350013), and by Natural Science Foundation Project of CQ CSTC (Grant No. CSTC, 2009BB4104), and by Fundamental Research Funds for the Central Universities (Grant No. XDJK2010B009). We are grateful to the anonymous referees for their suggestions.

References

1. Friend RH, Cymer RW, Holmes AB, Burroughes JH, Marks RN, Taliani C et al. (1999) Nature 397:121–128
2. Bernius MT, Inbasekaran M, O'Brien J, Wu W (2000) Adv Mater 12:1737–1750
3. Waser R (ed) (2003) Nanoelectronics and information technology-advanced electronic materials and novel devices. Wiley-VCH, Weinheim, p 917
4. Shirota Y, Kinoshita M, Noda T, Okumoto K, Ohara T (2000) J Am Chem Soc 122(44):11201–11202
5. Neher D (2001) Macromol Rapid Comm 22:1365–1385
6. Scherf U, List EJW (2002) Adv Mater 14:477–487
7. Babel A, Jenekhe SA (2003) 36: 7759–7764
8. Yu WL, Pei J, Huang W, Heeger AJ (2000) Adv Mater 12:828–831
9. Tang S, Liu MR, Gu C, Zhao Y, Lu P, Lu D et al. (2008) J Org Chem 73:4212–4218
10. Sanchez JC, Trogler WC (2008) J Mater Chem 18:3143–3156
11. Fu YQ, Sun MH, Wu YG, Bo ZS, Ma DG (2008) J Polym Sci Part A Polym Chem 46:1349–1356
12. Lin Y, Chen ZK, Ye TL, Dai YF, Ma DG, Ma Z, Liu QD, Chen Y (2010) Polymer 51:1270–1278
13. Marcus RA (1993) Angew Chem Int Ed Engl 32:1111–1121
14. Parr G, Yang W (1989) Density-functional theory of atoms and molecules. University Press, Oxford New York
15. Becke AD (1993) J Chem Phys 98:5648–5652
16. Lee C, Yang W, Parr RG (1988) Phys Rev B 37:785–789
17. Frisch MJ, Trucks GW, Schlegel HB, Scuseria GE, Robb MA, Cheeseman JR, Scalmani G, Barone V, Mennucci B, Petersson GA, Nakatsuji H et al. (2009) Gaussian 09, Revision A 02. Gaussian Inc, Wallingford, CT
18. Bader RFW (1990) Atoms in molecules, a quantum theory; International series of monographs in chemistry, vol 22. Oxford University Press, Oxford
19. PvR S, Maerker C, Dransfeld A, Jiao H, van Eikema Hommes NJR (1996) J Am Chem Soc 118:6317–6318
20. Shen W, Li M, He RX, Zhang JS, Lei W (2007) Polymer 48:3912–3918
21. Carpenter JE, Weinhold F (1988) J Mol Struct (THEOCHEM) 169:41–45
22. Reed AE, Curtiss LA, Weinhold F (1988) Chem Rev 88:899–926
23. Foster JP, Weinhold F (1980) J Am Chem Soc 102:7211–7218
24. Reed AE, Weinstock RB, Weinhold FJ (1985) J Chem Phys 83:735–746
25. O'Boyle NM, Vos JG (2005) GaussSum 1.0. Dublin City University. Available at http:gausssum.sourceforge.net
26. Herlem G, Lakard B (2004) J Chem Phys 120:9376–9382
27. Marcus RA (1993) Rev Mod Phys 65:599–610
28. Marcus RA, Eyring H (1964) Annu Rev Phys Chem 15:155–196
29. Hush NS (1958) J Chem Phys 28:962–972
30. Yang XD, Wang LJ, Wang CL, Long W, Shuai ZG (2008) Chem Mater 20:3205–3211
31. Wang FH, Yang XD, Li QK, Shuai ZG (2008) Org Electron 9:635–640
32. Troisi A, Orlandi G (2006) J Phys Chem A 110:4065–4070
33. Yin SW, Yi YP, Li QX, Yu G, Liu YQ, Shuai ZG (2006) J Phys Chem A 110:7183–7143
34. Köse ME, Mitchell WJ, Kopidakis N, Chang CH, Shaheen SE, Kim K, Rumbles G (2007) J Am Chem Soc 129:14257–14270
35. Nelsen SF, Trieber DA, Ismagilov RF, Teki Y (2001) J Am Chem Soc 123:5684–5694
36. Nelsen SF, Blomgren F (2001) J Org Chem 66:6551–6559
37. Lemaur V, Steel M, Beljonne D, Brédas JL, Cornil J (2005) J Am Chem Soc 127:6077–6086
38. Zou LY, Ren AM, Feng JK, Liu YL, Ran XQ, Sun CC (2008) J Phys Chem A 112:12172–12178
39. Tolbert LM (1992) Acc Chem Res 25:561–568
40. Fu YW, Shen W, Li M (2008) Polymer 49:2614–2620
41. PvR S, Jiao H, van Eikema Hommes NJR, Malkin VG, Malkina O (1997) J Am Chem Soc 119:12669–12670
42. PvR S, Jiao H (1996) Pure Appl Chem 68:209–218
43. Sista P, Nguyen H, Murphy JW, Hao J, Dei DK, Palaniappan K, Servello J, Kularatne RS, Gnade BE, Xue B, Dastoor PC, Biewer MC, Stefan MC (2010) Macromolecules 43:8063–8070
44. Tomasi J, Mennucci B, Cammi R (2005) Chem Rev 105:2999. doi:10.1021/cr9904009
45. Pedone A, Prampolini G, Monti S, Barone V (2011) Phys Chem Chem Phys 13:16689–16697
46. Matulis VE, Palagin DM, Ivashkevich OA (2010) Russ J Gen Chem 80:1078–1085

47. Sundholm D, Taubert S, Pichierri F (2010) Phys Chem Chem Phys 12:2751–2757
48. Litani-Barzilai I, Bulatov V, Gridin VV, Schechter I (2004) Anal Chim Acta 501:151–156
49. Lukeš V, Aquino A, Lischka H (2005) J Phys Chem A 109:10232–10238
50. Curioni A, Boero M, Andreoni W (1998) Chem Phys Lett 294:263–271
51. Wang I, Botzung-Appert E, Stéphan O, Ibanez A, Baldeck PL (2002) J Opt A Pure Appl Opt 4:S258–S260
52. Jia WL, Feng XD, Bai DR, Lu ZH, Wang S, Vamvounis G (2005) Chem Mater 17:164–179
53. Zou LY, Zhang ZL, Ren AM, Ran XQ, Feng JK (2010) Theor Chem Acc 126:361–369
54. Zou LY, Ren AM, Feng JK, Ran XQ (2009) J Phys Org Chem. doi:10.1002/poc.1565
55. Lin BC, Cheng CP, You ZQ, Hsu CP (2005) J Am Chem Soc 127:66–67
56. Gruhn NE, da Silva Filho DA, Bill TG, Malagoli M, Coropceanu V, Kahn A, Brédas JL (2002) J Am Chem Soc 124:7918–7919